

# CQ-DINO: Mitigating Gradient Dilution via Category Queries for Vast Vocabulary Object Detection

Zhichao Sun<sup>1,2</sup>, Huazhang Hu<sup>2</sup>, Yidong Ma<sup>2</sup>, Gang Liu<sup>2</sup>, Nemo Chen<sup>2</sup>, Xu Tang<sup>2</sup>, Yongchao Xu<sup>1\*</sup>  
<sup>1</sup>School of Computer Science, Wuhan University;  
<sup>2</sup>Xiaohongshu Inc.

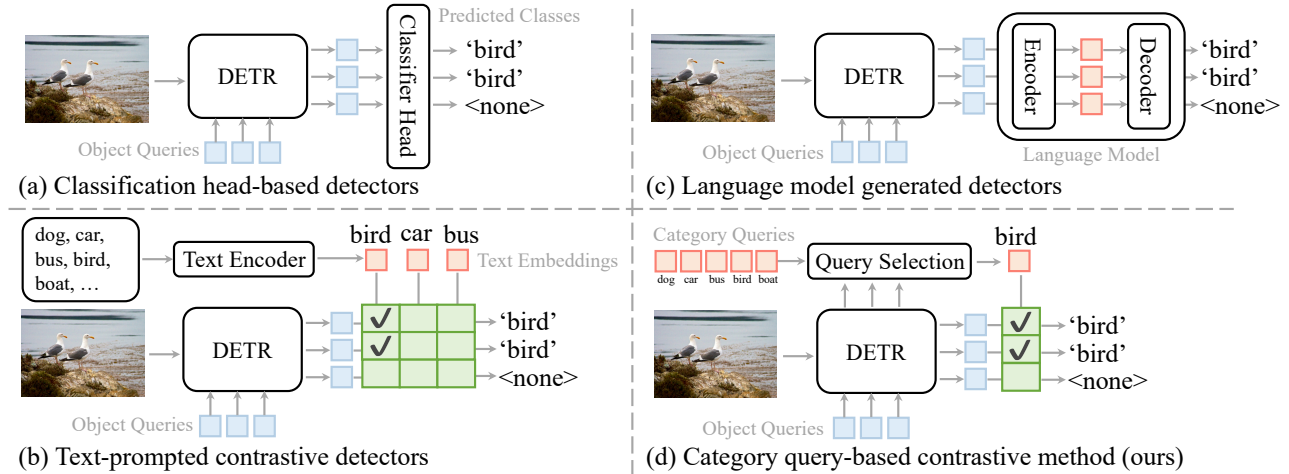


Figure 1. Comparison of category prediction mechanisms for vast vocabulary object detection. (a) Classification head-based detectors with fixed FFN layers face severe optimization challenges with increasing vocabulary size. (b) Text-prompted contrastive detectors leverage VLMs but require multiple inference passes for vast category lists. (c) Language model generated detectors enable open-ended detection but lack control over category granularity. (d) Our proposed CQ-DINO encodes categories as learnable category queries and leverages query selection to identify the most relevant categories in the image, achieving both scalability and improved performance.

## Abstract

With the exponential growth of data, traditional object detection methods are increasingly struggling to handle vast vocabulary object detection tasks effectively. We analyze two key limitations of classification-based detectors: **positive gradient dilution**, where rare positive categories receive insufficient learning signals, and **hard negative gradient dilution**, where discriminative gradients are overwhelmed by numerous easy negatives. To address these challenges, we propose **CQ-DINO**, a category query-based object detection framework that reformulates classification as a contrastive task between object queries and learnable category queries. Our method introduces image-guided query selection, which reduces the negative space by adaptively retrieving top-K relevant categories per image via cross-attention, thereby rebalancing gradient distributions and facilitating implicit hard example mining. Furthermore, CQ-DINO flexibly integrates explicit hierar-

chical category relationships in structured datasets (e.g., V3Det) or learns implicit category correlations via self-attention in generic datasets (e.g., COCO). Experiments demonstrate that CQ-DINO achieves superior performance on the challenging V3Det benchmark (surpassing previous methods by 2.1% AP) while maintaining competitiveness in COCO. Our work provides a scalable solution for real-world detection systems requiring wide category coverage. The dataset and code will be publicly at <https://github.com/RedAIGC/CQ-DINO>.

## 1. Introduction

With the rapid expansion of data, developing a robust AI system capable of large-scale object detection has become essential. This necessity is driven by real-world applications' increasing complexity and diversity, where AI must manage extensive vocabulary and dynamic environments.

Vast vocabularies inherently present hierarchical category structures, as illustrated by classification datasets like ImageNet [7] and Bamboo [48]. Recent detection benchmarks such as V3Det [37], featuring 13,204 object categories organized in hierarchical structures, highlight the magnitude of this challenge. While object detection has witnessed significant advancements [10, 17, 22, 27], scaling effectively to vast vocabularies remains a substantial challenge.

Classification head-based methods typically employ feed-forward networks (FFNs) with sigmoid activation and Focal loss [30] optimization. While these approaches succeed on benchmarks with limited categories such as COCO [19] (80 categories) and Objects365 [31] (365 categories), they face fundamental challenges and scalability in vast vocabulary settings. Recent benchmarks such as V3Det [37], featuring 13,204 object categories, highlight the challenges in vast vocabulary detection. Text-prompted contrastive methods leverage Vision-Language Models (VLMs) to achieve impressive performance in open-vocabulary [45] and visual grounding [44] tasks. These approaches inherit strong generalization capabilities by encoding target categories as text inputs to VLMs. However, they struggle to perform in vast vocabulary scenarios where the text input grows prohibitively long, limiting their practical applicability. Language model-generated methods address open-ended [18] object detection by employing language models to generate category labels without predefined inputs. While theoretically capable of detecting arbitrary objects, these approaches cannot reliably control the granularity of generated categories, creating a fundamental misalignment with practical detection requirements.

In this work, we first systematically analyze the challenges in vast vocabulary detection, focusing particularly on classification-based methods. Our analysis reveals two critical limitations: (1) **positive gradient dilution**, where the sparse positive categories receive insufficient gradient updates compared to the overwhelming negative categories, and (2) **hard negative gradient dilution**, where informative hard negative gradients get overwhelmed among numerous easy negative examples.

To tackle these challenges, we introduce category query-based contrastive detection (CQ-DINO), a DINO-based architecture that encodes categories as learnable queries. Our key insight is that **dynamic sparse category selection reduces negative space**. To this end, we introduce image-guided query selection that identifies relevant categories based on image content. We compute category-to-image similarity through cross-attention layers, followed by top-K selection. This allows us to retain only the most relevant categories for each image, typically a small fraction of the total vocabulary. This selection mechanism provides three crucial benefits: (1) it balances the ratio between positive and negative gradients, (2) it performs implicit hard mining

by selecting the most similar categories, and (3) it reduces memory and computational costs, making the framework scalable to extremely large vocabularies. The selected category queries then interact with image features to obtain object queries. From these object queries, bounding boxes are predicted through a cross-modality decoder. Final classifications are obtained using contrastive alignment between object queries and category queries.

The category query offers flexibility beyond traditional classification head-based methods, as it can easily encode inter-category correlations. For datasets with explicit category hierarchies like V3Det [37], we leverage the inherent tree structure to construct hierarchical category queries with an adaptive weight that balances local and hierarchical features. For datasets without explicit hierarchies (*e.g.*, COCO [19]), we use self-attention to learn correlations between categories implicitly.

We evaluate CQ-DINO on both the vast vocabulary V3Det dataset [37] and the standard COCO benchmark [19]. Our approach surpasses previous state-of-the-art methods on V3Det while maintaining competitive results on COCO compared to DETR-based detectors. Our method benefits from vast vocabulary detection while maintaining competitive results in limited vocabulary scenarios.

Our contributions can be summarized as follows:

- We systematically analyze the challenges in vast vocabulary object detection, identifying positive gradient dilution and hard negative gradient dilution as critical limitations of classification-based methods.
- We introduce learnable category queries that flexibly encode category correlations with efficient hierarchical tree construction for explicitly modeling category relationships in vast vocabulary scenarios.
- We develop an image-guided query selection module that dynamically identifies relevant categories per image, effectively addressing the identified limitations while significantly reducing computational complexity.

## 2. Related Work

### 2.1. Vast vocabulary object detection

The progression of object detection datasets reveals a trend toward increasingly expansive vocabularies: from small-scale benchmarks like PASCAL VOC [9] (20 classes) to medium-scale datasets such as Objects365 [31] (365 classes), to large-vocabulary benchmarks like LVIS [11] (1,203 classes). Wang et al. [37] introduce the first vast vocabulary object detection dataset, V3Det. V3Det encompasses 13,204 classes organized in hierarchical structures and presents new scalability challenges.

While the LVIS dataset serves as a large-vocabulary detection benchmark, it primarily presents challenges related to long-tail distributions (28% classes appear in fewer

than 11 images). To address these challenges, several loss functions have been proposed, including Equalization loss [32, 33, 50] and SeeSaw loss [36], which reweight per-class losses by balancing gradients or sample frequencies. Additionally, Yang et al. [41], and Detic [53] incorporate additional image-level datasets with fine-grained classes to improve detection performance for rare categories.

The V3Det Challenge [38] has inspired several pipelines for vast vocabulary object detection. The MixPLv2 [38] model designs a semi-supervised pipeline that leverages V3Det as the labeled dataset and Objects365 [31] as the unlabeled dataset. RichSem-DINO-FocalNet [38] utilizes the RichSem-DINO detection framework [24], incorporating FocalNet-Huge [42] as its backbone pretrained on the Objects365 dataset [31]. In recent work, Prova [4] proposes specifically for V3Det and introduces detailed image and text prototypes for classification. However, these methods still rely on fundamentally similar classification architectures, raising questions about their viability for even larger vocabularies beyond tens of thousands of categories.

## 2.2. Classification-based detectors

Object detection architectures typically employ feedforward networks (FFNs) as fixed classification heads for category prediction. Traditional two-stage detectors [2, 12, 27] first generate class-agnostic proposals through Region Proposal Networks (RPNs), then classify these regions using FFN-based classifiers. In contrast, one-stage detectors [8, 30, 35] streamline detection by directly predicting bounding boxes and categories in a single step.

The transformer-based DETR [3] reformulated object detection as a set prediction problem using learnable queries. However, it suffered from slow convergence. Subsequent works [13, 16, 20, 21, 25, 39, 46, 54] address these limitations. For example, Deformable DETR [54] proposes multi-scale deformable attention with sparse spatial sampling. DINO [46] achieves impressive performance by leveraging contrastive query denoising and mixed query selection strategies. Despite these architectural advances, existing methods fundamentally rely on classification heads with activation functions, trained using Focal loss [30] or Cross-Entropy loss [49]. This design paradigm inherently limits scalability and poses optimization challenges when scaling up to vast vocabulary scenarios.

With the rapid development of multi-modal models, visual and textual information integration has become increasingly seamless. Recent vision-language models enable text-prompted object detection by aligning visual features with text features. These methods achieve impressive performance in open-vocabulary and visual grounding tasks. GLIP [17] pioneers this approach by establishing contrastive learning between image regions and textual phrases using large-scale image-text pairs. Grounding

DINO [22] further enhances cross-modal alignment through the early fusion of vision and language features. Similarly, DetCLIP [43] and RegionCLIP [51] leverage image-text pairs with pseudo-labels to expand region-level semantic understanding for stronger generalization ability.

However, these text-prompted methods face fundamental limitations when scaling to vast vocabularies, primarily due to their restricted text token capacity. For instance, GLIP [17] and Grounding DINO [22] limit input prompts to approximately 128 tokens, which corresponds to roughly 40 categories per inference pass. Consequently, detecting all classes in a dataset like V3Det [37] (13,204 categories) would require over 331 sequential inference passes per image. Therefore, these methods are computationally impractical for real-time applications and are not feasible for large-scale vocabulary object detection.

## 2.3. Generative detectors

In recent years, the success of generative models has driven significant advancements in multimodal large language models (MLLMs), inspiring detection approaches that leverage their powerful visual understanding and generative capabilities. Although some multi-modal large models (e.g., InternVL [5], Qwen-VL [1], Gemini [34]) have demonstrated preliminary object detection capabilities, they still lack the ability for precise detection. To address this limitation, recent works [10, 15, 18, 37, 40] have utilized LLMs specifically as category generators rather than direct detectors. GenerateU [18] employs a T5 model [6] to decode object categories from visual features, thereby framing detection as a text-generation task. Similarly, LLMDet [10] and ChatRex [15] utilize instruction-tuned LLMs to predict object categories from image features.

Although open detection is theoretically possible, these generation methods have inconsistencies with the detection requirements due to the uncontrollable granularity of the generated categories. For example, when regions contain the term “Persian cat”, these methods may output a more general term “cat”, introducing ambiguity and reducing the accuracy required for fine-grained detection tasks.

## 3. Method

### 3.1. Challenges in vast vocabulary detection

Existing methods for vast vocabulary object detection with  $C$  categories ( $C > 10^4$ ), particularly those employing sigmoid-based classifiers with Focal loss [30], face fundamental optimization challenges. To systematically analyze these issues, we consider a simplified formulation using Cross-Entropy loss with sigmoid activation, revealing two critical limitations:

**1) Positive gradient dilution.** In vast vocabulary detection, the gradient signal for positive classes is overwhelmed by

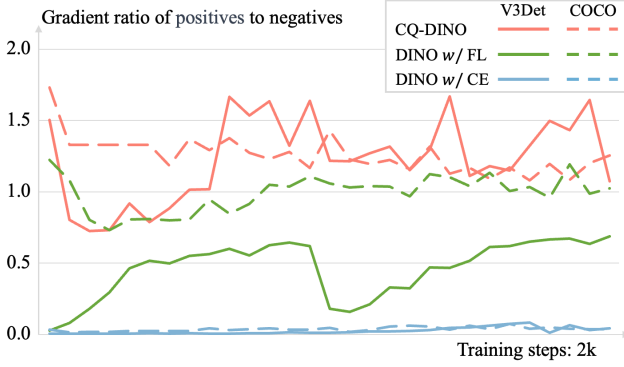


Figure 2. Positive-to-negative gradient ratio comparing CQ-DINO against DINO with Focal loss (FL) and Cross-Entropy loss (CE) on V3Det and COCO datasets, showing the initial 2k training iterations where differences are most evident.

the aggregated negative gradients. Let  $z_c$  denote the logit for class  $c$  and  $y_c \in \{0, 1\}$  its ground-truth label. The gradient of the Cross-Entropy loss  $\mathcal{L}$  with respect to  $z_c$  is:

$$\nabla_{z_c} \mathcal{L} = \sigma(z_c) - y_c, \quad (1)$$

where  $\sigma(\cdot)$  is the sigmoid function. For a positive class  $c^+$  ( $y_{c^+} = 1$ ), the gradient magnitude is  $|\nabla_{z_{c^+}} \mathcal{L}| = 1 - \sigma(z_{c^+})$ , while for negatives  $c^-$  ( $y_{c^-} = 0$ ), it is  $|\nabla_{z_{c^-}} \mathcal{L}| = \sigma(z_{c^-})$ .

The total negative gradient magnitude grows linearly with category count  $C$ :

$$\|\nabla_{z_{c^+}} \mathcal{L}\| \ll \sum_{c^- \neq c^+} \|\nabla_{z_{c^-}} \mathcal{L}\| \approx (C - 1) \cdot \epsilon, \quad (2)$$

where  $\epsilon = \mathbb{E}[\sigma(z_{c^-})]$  represents the average activation probability of negative classes. The positive-to-negative gradient ratio  $\rho$  becomes:

$$\rho = \frac{\|\nabla_{z_{c^+}} \mathcal{L}\|}{\sum_{c^- \neq c^+} \|\nabla_{z_{c^-}} \mathcal{L}\|} \approx \frac{1 - \sigma(z_{c^+})}{(C - 1) \cdot \mathbb{E}[\sigma(z_{c^-})]} \propto \frac{1}{C \cdot \epsilon}. \quad (3)$$

As  $C$  increases in vast category scenarios (e.g.,  $C > 10^4$ ),  $\rho \rightarrow 0$  causes positive gradients to be suppressed during optimization. This fundamentally hinders the model’s ability to learn from positive examples.

**2) Hard negative gradient dilution.** The massive negative space leads to gradient dominance by easily classified negatives rather than informative hard negatives. Let  $\mathcal{H}$  denote the set of hard negative classes with  $\mathbb{E}[\sigma(z_{c^h})] = \epsilon^h$  for  $c^h \in \mathcal{H}$ . The ratio of hard negative gradients to total negative gradients is:

$$\eta = \frac{\sum_{c^h \in \mathcal{H}} |\nabla_{z_{c^h}} \mathcal{L}|}{\sum_{c^- \neq c^+} |\nabla_{z_{c^-}} \mathcal{L}|} \approx \frac{N_h}{C} \cdot \frac{\epsilon^h}{\epsilon}, \quad (4)$$

where  $N_h$  is the number of hard negatives. As  $C$  exceeds  $10^4$ ,  $\eta \rightarrow 0$  due to the  $\frac{1}{C}$  term, making hard negatives diluted in gradient updates.

Fig. 2 demonstrates these theoretical challenges. The gradient ratio for the V3Det dataset (13,204 classes) is smaller than for the COCO dataset (80 classes), revealing the inherent difficulty in vast vocabulary object detection. While Focal loss partially mitigates these issues by down-weighting easy negatives, the gradient ratio for V3Det remains around 0.5 compared to approximately 1.0 for COCO, indicating that gradient imbalance persists despite these improvements. We provide a comprehensive experimental analysis of Focal loss performance and limitations in Section 4.5.

### 3.2. CQ-DINO

Our key insight is that dynamically selecting a sparse category subset  $S \subset \{1, \dots, C\}$  simultaneously addresses both gradient dilution challenges through gradient magnitude rebalancing and adaptive hard negative mining. As shown in Fig. 3, CQ-DINO consists of three key components:

**1) Learnable category queries with correlation encoding.** We initialize learnable category queries  $Q_{cat} \in \mathbb{R}^{B \times C \times D}$  using the OpenCLIP [26] text encoder, where  $B$  is the batch size,  $C$  denotes the total number of categories, and  $D$  is the embedding dimension. These category queries enable flexible encoding of category correlations through self-attention or hierarchical tree construction (Sec. 3.4).

**2) Image-guided query selection.** Given image features  $F_{img} \in \mathbb{R}^{B \times D \times H' \times W'}$  from the image encoder, we compute the similarity between  $F_{img}$  and  $Q_{cat}$  through multi-head cross-attention modules. For each image, we select the top- $C'$  most relevant queries ( $C' \ll C$ , typically  $C' = 100$  for  $C > 10^4$ ), ensuring that the target class  $c^+$  and its semantically confusing negative classes are preserved. This selection process rebalances the gradients and implicitly performs hard negative mining.

**3) Feature enhancer and cross-modality decoder.** The selected category queries  $Q'_{cat} \in \mathbb{R}^{B \times C' \times D}$  along with image features  $F_{img}$  are processed through GroundingDINO [22] components. First, the feature enhancer module fuses category queries and image features. Next, object queries are generated through language-guided query selection. Finally, detection outputs are produced by the cross-modality decoder and contrastive alignment between object queries and selected category queries.

### 3.3. Image-guided query selection

The core innovation of CQ-DINO is our image-guided category selection module, illustrated in Fig. 4. Our selection module employs cross-attention between category queries  $Q_{cat}$  and image features  $F_{img}$ . Here,  $Q_{cat}$  serve as queries (Q), while  $F_{img}$  provide keys (K) and values (V). The



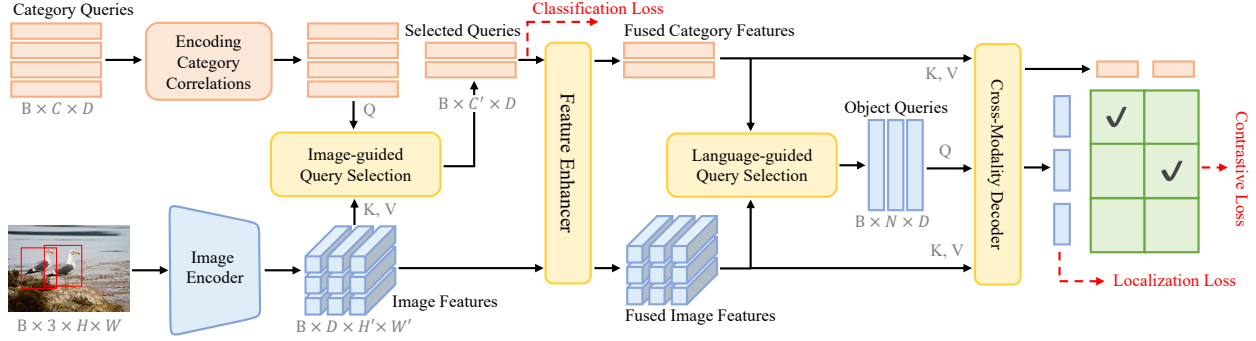


Figure 3. Overview of the CQ-DINO framework for vast vocabulary object detection. Key components include: (1) Learnable category queries enhanced with hierarchical tree construction for semantic relationship modeling; (2) Image-guided query selection that identifies the most relevant category queries; (3) Feature enhancer and cross-modality decoder (adapted from GroundingDINO [22]) that processes object queries with contrastive alignment between object queries and selected category queries.

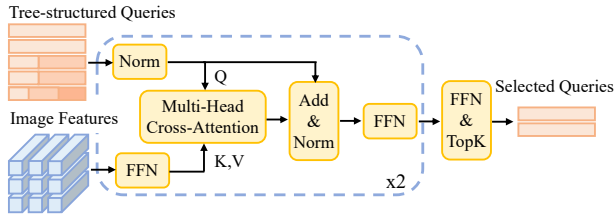


Figure 4. Illustration of image-guided query selection module.

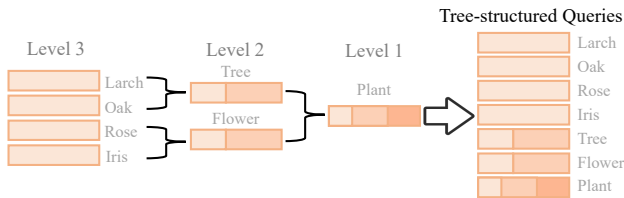


Figure 5. Hierarchical tree construction for category queries.

cross-attention layer establishes category-to-image correlations through similarity computation. Then, we apply TopK selection to retain only the top- $C'$  categories ( $C' \ll C$ ) based on activation values. We supervise this selection using Asymmetric loss [29], which serves as a multi-class classification loss.

The selection rebalances the positive-to-negative gradient ratio. Let  $\rho$  and  $\rho'$  denote the original and revised positive-to-negative gradient ratios, respectively:

$$\frac{\rho'}{\rho} = \frac{\sum_{c^-} \|\nabla_{z_{c^-}} \mathcal{L}\|}{\sum_{c^- \in S} \|\nabla_{z_{c^-}} \mathcal{L}\|} \approx \frac{C}{C'}. \quad (5)$$

For a typical setting ( $C > 10^4$ ,  $C' = 100$ ), this achieves a  $100\times$  gradient rebalancing factor. Our design provides three benefits: **1) Gradient rebalancing.** By filtering out easy negative categories, our selection module improves the influence of gradients from positive examples. **2) Adaptive hard negative mining.** The selection mechanism en-

sures that retained negative categories exhibit high semantic relevance to the image content, naturally implementing hard negative mining. **3) Scalable computation.** Processing only  $C'$  categories reduces memory consumption and computational cost, making the framework scalable to extremely large vocabularies.

### 3.4. Encoding category correlations

A key advantage of our category query approach is the capacity to model complex semantic relationships among categories, which is difficult for traditional classification head-based methods. We propose two complementary strategies for encoding category correlations.

**Explicit hierarchical tree construction.** For hierarchical datasets like V3Det [37], we introduce hierarchical tree construction, as shown in Fig. 5. The process begins at leaf nodes and progressively integrates hierarchical information upward through the category tree. For each parent node  $v$  with children  $\mathcal{C}(v)$ , its new query  $Q'_v$  is a combination of its original query  $Q_v$  and the mean pooling of all direct child nodes. Leaf nodes retain their original features directly since they have no children.

$$Q'_v = (1 - \alpha_v) \cdot Q_v + \alpha_v \cdot \frac{1}{|\mathcal{C}(v)|} \sum_{c \in \mathcal{C}(v)} Q_c, \quad (6)$$

where  $\alpha_v \in [0, 1]$  balances local and hierarchical features.

$$\alpha_v = w \left( 1 + \frac{\log(n_v + 1)}{\log(N_{\max} + 1)} \right), \quad (7)$$

where  $n_v$  is the child count for node  $v$ ,  $N_{\max}$  is the maximum child count across the tree, and  $w \in [0, 0.5]$  is a hyperparameter (default: 0.3). This adaptive weight  $\alpha_v$  ensures parent nodes with more descendants incorporate more collective knowledge, while nodes with fewer children maintain stronger individual semantics.

Building upon this structural design, we introduce a masking strategy during classification loss computation to mitigate hierarchical ambiguity. If any child category exists in the ground truth, its parent nodes are excluded from the classification loss. This prevents conflicting supervision signals for semantically related categories, such as suppressing “vehicle” when “car” is annotated.

**Implicit relation learning.** For categories without explicit hierarchical structure, we employ a self-attention mechanism to learn category relationships. This allows semantically related categories to influence each other’s representations based on learned attention patterns.

## 4. Experiments

### 4.1. Datasets

We conduct experiments on two detection benchmarks:

- (1) V3Det [37]: A vast vocabulary detection dataset containing 13,204 categories with 183k training and 30k validation images. This dataset represents our primary benchmark for evaluating vast vocabulary detection capabilities.
- (2) COCO val2017 [19]: A standard benchmark dataset with 80 common object categories comprising 118k training and 5k validation images. We include this dataset to verify the effectiveness of our method in limited vocabulary scenarios.

### 4.2. Implementation details

All experiments are conducted on 8 NVIDIA A100-40G GPUs with a total batch size of 16. We follow baseline methods’ original configurations for fair comparison. We implement three Swin Transformer [23] variants as backbones: Swin-B (ImageNet-1k [7] pre-trained), Swin-B-22k (ImageNet-22k pre-trained), and Swin-L (ImageNet-22k pre-trained). Our category queries are initialized using text embeddings from CLIP-ViT-L [26]. To handle dataset-specific vocabulary variations, we employ 100 category queries for V3Det and 30 queries for COCO, aligned with their respective category sizes. We derive the hierarchical tree structure from V3Det’s category taxonomy for tree construction. For the implicit relation learning, we employ a standard 8-head self-attention module.

The training objective combines multiple loss terms with the following weights: classification loss (Asymmetric loss [29], weight=1.0), contrastive alignment (Focal loss [30], weight=1.0), bounding box regression (L1 loss, weight=5.0), and GIoU loss [28] (weight=2.0), as in GroundingDINO [22]. We employ Hungarian matching following GroundingDINO [22] with identical matching costs for the object-to-query assignment. To stabilize training, we use a two-stage training approach. In the first stage, we pre-train the category queries, image encoder, and image-guided query selection module for 10 epochs. This creates

Method	Epochs	Backbone	$AP$	$AP_{50}$	$AP_{75}$
ATSS [47]	24	Swin-B	7.6	8.9	8.0
FCOS [35]	24	Swin-B	21.0	24.8	22.3
Faster R-CNN [27]	24	Swin-B	37.6	46.0	41.1
CenterNet2 [52]	24	Swin-B	39.8	46.1	42.4
Cascade R-CNN [2]	24	Swin-B	42.5	49.1	44.9
Deformable DETR [54]	50	Swin-B	42.5	48.3	44.7
DINO [46]	24	Swin-B	42.0	46.8	43.9
Prova [4]	24	Swin-B	44.5	49.9	46.6
CQ-DINO (Ours)	24	Swin-B	<b>46.3</b>	<b>51.5</b>	<b>48.4</b>
<hr/>					
DINO [46]	24	Swin-B-22k	43.4	48.4	45.4
Prova [4]	24	Swin-B-22k	50.3	56.1	52.6
CQ-DINO (Ours)	24	Swin-B-22k	<b>52.3</b>	<b>57.7</b>	<b>54.6</b>
<hr/>					
DINO [46]	24	Swin-L	48.5	54.3	50.7
Prova [4]	24	Swin-L	50.9	57.2	53.2
CQ-DINO (Ours)	24	Swin-L	<b>53.0</b>	<b>58.4</b>	<b>55.4</b>

Table 1. Comparison with state-of-the-art methods on the V3Det validation set. Best results in each group are highlighted in **bold**.

Method	Epochs	Backbone	$AP$	$AP_S$	$AP_M$	$AP_L$
H-Def-DETR [14]	36	Swin-L	57.1	39.7	61.4	73.4
Relation-DETR [13]	12	Swin-L	57.8	41.2	62.1	<b>74.4</b>
DINO [46]	36	Swin-L	58.0	41.3	62.1	73.6
Rank-DETR [25]	36	Swin-L	58.2	42.4	<b>62.2</b>	73.6
CQ-DINO (ours)	24	Swin-L	<b>58.5</b>	<b>42.5</b>	62.1	74.0

Table 2. Comparison with state-of-the-art DETR variants on COCO val2017 (best results reported from original papers).

a high initial recall of target categories before fine-tuning the complete detection pipeline in the second stage.

### 4.3. Experimental results

**Performance on vast vocabulary detection.** Tab. 1 presents our comparison with state-of-the-art methods on the V3Det [37] benchmark. CQ-DINO consistently outperforms all previous approaches across different backbone configurations. With the Swin-B backbone, CQ-DINO achieves 46.3% AP, outperforming general detection methods like Deformable DETR [54] by 3.8% AP and DINO [46] by 4.3% AP. More importantly, CQ-DINO surpasses Prova [4], a specialized vast vocabulary detection method, by 1.8% AP. When integrated with the Swin-B-22k backbone, CQ-DINO achieves 52.3% AP, outperforming Prova by 2.0% AP. With the Swin-L backbone, CQ-DINO achieves 53.0% AP. The consistent improvements across different backbones demonstrate that CQ-DINO effectively addresses vast vocabulary detection challenges.

**Performance on standard detection benchmark.** Tab. 2 compares our method with state-of-the-art approaches on COCO val2017. Despite being primarily designed for vast vocabulary scenarios, CQ-DINO achieves competitive performance, reaching 58.5% AP, comparable with recent DETR-based methods. To ensure a fair comparison, we re-

ECC	IGQS	$AP$	$AR_{100}^C$	FPS
		<i>Out</i>	<i>Of</i>	<i>Memory</i>
TC		<i>Out</i>	<i>Of</i>	<i>Memory</i>
	✓	51.1	80.9	<b>6.7</b>
SA	✓	51.3 (↑ 0.2)	75.5 (↓ 5.4)	6.5 (↓ 0.2)
TC	✓	<b>52.3</b> (↑ 1.2)	<b>83.3</b> (↑ 2.4)	6.6 (↑ 0.1)

Table 3. Ablation study on the effectiveness of encoding category correlations (ECC) and image-guided query selection (IGQS) components in CQ-DINO on V3Det dataset using Swin-Base-22k backbone. SA denotes Self-Attention module and TC refers to hierarchical tree construction. Metrics include AP, category-level recall ( $AR_{100}^C$ ), and inference speed (FPS). The absence of IGQS results in CUDA memory overflow.

port the best results in their original papers. Results demonstrate that our method achieves gradient rebalancing and adaptive hard mining as in limited vocabulary scenarios.

#### 4.4. Ablation studies

We conduct comprehensive ablation studies to analyze the effectiveness of each component in the proposed CQ-DINO. All experiments are performed on the V3Det dataset using a Swin-B-22k backbone unless otherwise specified.

**Effect of each component in CQ-DINO.** Tab. 3 presents component contributions using  $AP$  and  $AR_{100}^C$  (category-level average recall with 100 selected queries).

Image-guided query selection resolves memory constraints. Without this component, the baseline fails to run on A100-40G GPUs even with batch size 1 due to high category processing demands.

The category query framework shows superior flexibility over conventional detection heads in modeling inter-category relationships. Tree construction delivers gains of 1.2% AP and 2.4%  $AR_{100}^C$  through explicit hierarchical relationship modeling. self-attention’s implicit approach achieves marginal +0.2% AP but reduces  $AR_{100}^C$ . This stems from difficulties learning complex relationships across 13k+ categories. Tree construction introduces zero parameters with only 0.1 FPS overhead, while self-attention adds 2.36M parameters and 0.2 FPS overhead.

While Tab. 3 shows that explicit tree construction outperforms self-attention on V3Det’s vast category space, we conduct further experiments on COCO (Table 6). Results reveal that self-attention contributes meaningful 0.2% AP and 0.9%  $AR_{30}^C$  improvements on datasets with fewer categories. Both experiments validate the effectiveness of encoding category correlations, with the optimal approach depending on the scale of the category space.

**Impact of category query count.** Tab. 4 examines how varying the number of category queries (50/100/200) affects performance. As expected, increasing the number of queries improves  $AR_{100}^C$  at the cost of lower inference

Query Count	$AP$	$AR^C$	FPS
50	51.8	78.4	<b>6.9</b>
100	<b>52.3</b>	83.3	6.6
200	52.2	<b>87.5</b>	5.9

Table 4. Ablation study with different numbers of selected category queries in CQ-DINO on V3Det.

Method	$AP$	$AP_{50}$	$AP_{75}$	$AR_{100}^C$
Fixed weight (0.5)	51.9	57.4	54.3	82.3
Ours ( $\alpha_v$ )	<b>52.3</b>	<b>57.7</b>	<b>55.4</b>	<b>83.3</b>

Table 5. Ablation study on adaptive weighting in tree construction.

Method	$AP$	$AR_{30}^C$	Params (M)
CQ-DINO w/o SA	58.3	98.2	<b>244.3</b>
CQ-DINO w/ SA	<b>58.5</b> (↑ 0.2)	<b>99.1</b> (↑ 0.9)	246.7 (+2.4)

Table 6. Ablation study on Self-Attention module (SA) in CQ-DINO on the COCO dataset.

Method	Params/Cat. (K)	Memory/Cat. (kB)	Max Cats. (k)
DINO [46]	2.1	8.9	100
CQ-DINO	0.8	2.7	130

Table 7. Scalability comparison of CQ-DINO with DINO on A100 40G GPU using Swin-B-22k backbone, showing per-category parameters (K), CUDA memory consumption (kB), and maximum supported category capacity (k).

speed. However, simply maximizing query count is not optimal. With too many queries, the gradient imbalance between positive and negative examples becomes problematic. Our experiments show that 100 queries achieve optimal balance between detection and computational efficiency for V3Det. For COCO dataset experiments, 30 queries are sufficient, achieving 99.1%  $AR_{30}^C$ .

#### Effectiveness of adaptive weighting in tree construction.

Tab. 5 shows the importance of our adaptive weighting strategy compared to a fixed weight of 0.5. This approach adjusts weights based on the varying number of child categories for each parent node in the hierarchy. Results show our adaptive approach outperforms fixed weighting.

#### 4.5. Discussion

**Scalability of CQ-DINO.** Tab. 7 analyzes the scaling efficiency of CQ-DINO compared to DINO for vast vocabulary detection. Our method requires only 0.8K parameters per category, representing a 62% reduction from DINO’s 2.1K parameters. For runtime memory consumption, CQ-DINO uses 2.7KB CUDA memory per category. To evaluate practical scalability limits, we test the maximum category support on an A100-40G GPU using Swin-B-22k backbone

Method	Backbone	AP	AP <sub>50</sub>	AP <sub>75</sub>
GenerateU [18]	Swin-L&T5-B	0.4	0.5	0.4
ChatRex [15]	Swin-L&ChatRex-7B	1.3	1.5	1.4
*GenerateU* [18]	Swin-L&T5-B	17.2	22.4	17.7
DINO [46]	Swin-L	48.5	54.4	50.7
CQ-DINO (Ours)	Swin-L	<b>53.0</b>	<b>58.4</b>	<b>55.4</b>

Table 8. Performance of generated-based methods on V3Det dataset. We report zero-shot performance using their most powerful models. The line marked with \* \* represents GenerateU finetuned on the V3Det dataset.

$\gamma \backslash \alpha$	0.25	0.35	0.50	0.75
2	43.4	45.1	<b>47.4</b>	-
3	43.7	43.9	45.1	-
5	-	-	-	-

Table 9. Focal loss parameter analysis in DINO using Swin-B-22k backbone. AP scores (%) compare different  $\alpha$  and  $\gamma$  combinations. Dashes “-” indicate unstable training configurations.

with a single  $800 \times 1333$  resolution image. CQ-DINO supports detection of up to 130k categories, surpassing DINO’s 100k limit. Experiments validate that CQ-DINO enables applications with extremely larger vocabularies.

**Limitations of generation-based methods.** We evaluate generation-based methods on the V3Det dataset in Tab. 8. Following the evaluation protocol from GenerateU [18], we compute semantic similarity between generated category embeddings and V3Det category embeddings, selecting the highest similarity match as the final prediction. Our experiments reveal poor performance: GenerateU [18] achieves only 0.4% AP, while the more recent ChatRex [15] performs just 1.3% AP. This highlights a fundamental limitation: *generation-based methods struggle to control the granularity of generated categories, creating semantic misalignments with the specific requirements of detection tasks.* Furthermore, even when we finetune GenerateU on V3Det data, the resulting performance (17.2% AP) still exhibits a substantial gap compared to classification-head methods.

**Focal loss parameter analysis.** As analyzed in Sec. 3.1, vast vocabulary detection suffers from gradient dilution challenges. Focal loss (FL) [30] mitigates this via adaptive weighting with hyperparameters  $\alpha$  and  $\gamma$ . Theoretically,  $\alpha$  balances positive/negative sample contributions, where increasing  $\alpha$  enhances the model’s ability to handle more categories. Factor  $\gamma$  focuses learning on hard negatives, where increasing  $\gamma$  improves the mining of hard examples.

Tab. 9 evaluates FL configurations on DINO with a Swin-B-22k backbone. The baseline [37] ( $\alpha = 0.25$ ,

Method	Backbone	AP	AP <sub>50</sub>	AP <sub>75</sub>
DINO	Swin-B	42.0	46.8	43.9
‡ DINO	Swin-B	38.7 ( $\downarrow$ 3.3)	43.7 ( $\downarrow$ 3.1)	40.4 ( $\downarrow$ 3.5)
CQ-DINO	Swin-B	<b>46.3</b>	<b>51.5</b>	<b>48.4</b>
DINO	Swin-B-22k	43.4	48.4	45.4
‡ DINO	Swin-B-22k	47.4 ( $\uparrow$ 4.0)	53.3 ( $\uparrow$ 4.9)	49.7 ( $\uparrow$ 4.3)
CQ-DINO	Swin-B-22k	<b>52.3</b>	<b>57.7</b>	<b>54.6</b>
DINO	Swin-L	48.5	54.3	50.7
‡ DINO	Swin-L	50.1 ( $\uparrow$ 1.6)	56.3 ( $\uparrow$ 2.0)	52.4 ( $\uparrow$ 1.7)
CQ-DINO	Swin-L	<b>53.0</b>	<b>58.4</b>	<b>55.4</b>

Table 10. Performance comparison between standard DINO ( $\alpha = 0.25$ ,  $\gamma = 2$ ), ‡ DINO with modified Focal loss parameters ( $\alpha = 0.50$ ,  $\gamma = 2$ ), and the proposed CQ-DINO.

$\gamma = 2$ ) achieves 43.4% AP. We observe training instability for  $\gamma \geq 5$  or  $\alpha \geq 0.75$ . Optimal performance (47.2% AP, +4.0% over baseline) occurs at  $\gamma = 2$  and  $\alpha = 0.5$ , confirming that proper parameter tuning can substantially benefit vast vocabulary detection.

Interestingly, when examining parameter transferability across architectures in Tab. 10, we find that this optimal setting does not generalize well. The same parameters ( $\alpha = 0.5$ ,  $\gamma = 2$ ) lead to performance degradation of 3.3% AP for Swin-B backbone compared to default configuration ( $\alpha = 0.25$ ,  $\gamma = 2$ ). However, they increase the performance by 4.0% AP and 1.6% AP for Swin-B-22k and Swin-L backbones, respectively. These findings show that while Focal loss addresses gradient dilution issues, its optimal configuration requires careful parameter tuning.

#### 4.6. Limitation

While CQ-DINO achieves improvement in vast vocabulary object detection, several limitations need future exploration. First, our detection performance depends on the recall capability of our first-stage category query selection. The detector cannot recover them later if relevant categories are not included in the top-K selected queries. Fortunately, our approach achieves 83.3% AR, ensuring this component does not constitute a performance bottleneck in practice. Second, the two-stage training paradigm introduces additional complexity to the training pipeline. This separate optimization process could potentially limit the performance.

### 5. Conclusion

In this work, we analyze the challenges in vast vocabulary detection: positive gradient dilution and hard negative gradient dilution. To address these limitations, we propose CQ-DINO with two core innovations: (1) learnable category queries that encode category correlations, and (2) image-guided query selection that reduces negative space while performing adaptive hard negative min-



ing. CQ-DINO demonstrates superior performance on the V3Det benchmark and exhibits strong scalability to larger vocabularies. In the future, we will explore the flexibility of category queries for open-vocabulary detection and incremental learning scenarios.

## References

- [1] Jinze Bai, Shuai Bai, Yunfei Chu, Zeyu Cui, Kai Dang, Xiaodong Deng, Yang Fan, Wenbin Ge, Yu Han, Fei Huang, et al. Qwen technical report. *arXiv preprint arXiv:2309.16609*, 2023. 3
- [2] Zhaowei Cai and Nuno Vasconcelos. Cascade R-CNN: High quality object detection and instance segmentation. *IEEE Trans. Pattern Anal. Mach. Intell.*, 43(5):1483–1498, 2019. 3, 6
- [3] Nicolas Carion, Francisco Massa, Gabriel Synnaeve, Nicolas Usunier, Alexander Kirillov, and Sergey Zagoruyko. End-to-end object detection with transformers. In *Eur. Conf. Comput. Vis.*, pages 213–229, 2020. 3
- [4] Yitong Chen, Wenhao Yao, Lingchen Meng, Sihong Wu, Zuxuan Wu, and Yu-Gang Jiang. Comprehensive multi-modal prototypes are simple and effective classifiers for vast-vocabulary object detection. In *Proc. AAAI Conf. Artif. Intell.*, 2025. 3, 6
- [5] Zhe Chen, Jiannan Wu, Wenhao Wang, Weijie Su, Guo Chen, Sen Xing, Muyan Zhong, Qinglong Zhang, Xizhou Zhu, Lewei Lu, et al. InternVL: Scaling up vision foundation models and aligning for generic visual-linguistic tasks. In *IEEE Conf. Comput. Vis. Pattern Recog.*, pages 24185–24198, 2024. 3
- [6] Hyung Won Chung, Le Hou, Shayne Longpre, Barret Zoph, Yi Tay, William Fedus, Yunxuan Li, Xuezhi Wang, Mostafa Dehghani, Siddhartha Brahma, et al. Scaling instruction-finetuned language models. *Journal of Machine Learning Research*, 25(70):1–53, 2024. 3
- [7] Jia Deng, Wei Dong, Richard Socher, Li-Jia Li, Kai Li, and Li Fei-Fei. ImageNet: A large-scale hierarchical image database. In *IEEE Conf. Comput. Vis. Pattern Recog.*, pages 248–255, 2009. 2, 6
- [8] Kaiwen Duan, Song Bai, Lingxi Xie, Honggang Qi, Qingming Huang, and Qi Tian. CenterNet: Keypoint triplets for object detection. In *Int. Conf. Comput. Vis.*, pages 6569–6578, 2019. 3
- [9] Mark Everingham, SM Ali Eslami, Luc Van Gool, Christopher KI Williams, John Winn, and Andrew Zisserman. The pascal visual object classes challenge: A retrospective. *Int. J. Comput. Vis.*, 111:98–136, 2015. 2
- [10] Shenghao Fu, Qize Yang, Qijie Mo, Junkai Yan, Xihan Wei, Jingke Meng, Xiaohua Xie, and Wei-Shi Zheng. LLMDet: Learning strong open-vocabulary object detectors under the supervision of large language models. *arXiv preprint arXiv:2501.18954*, 2025. 2, 3
- [11] Agrim Gupta, Piotr Dollar, and Ross Girshick. LVIS: A dataset for large vocabulary instance segmentation. In *IEEE Conf. Comput. Vis. Pattern Recog.*, pages 5356–5364, 2019. 2
- [12] Kaiming He, Georgia Gkioxari, Piotr Dollár, and Ross Girshick. Mask R-CNN. In *Int. Conf. Comput. Vis.*, pages 2961–2969, 2017. 3
- [13] Xiuquan Hou, Meiqin Liu, Senlin Zhang, Ping Wei, Badong Chen, and Xuguang Lan. Relation DETR: Exploring explicit position relation prior for object detection. In *Eur. Conf. Comput. Vis.*, pages 89–105, 2024. 3, 6
- [14] Ding Jia, Yuhui Yuan, Haodi He, Xiaopei Wu, Haojun Yu, Weihong Lin, Lei Sun, Chao Zhang, and Han Hu. Detsr with hybrid matching. In *IEEE Conf. Comput. Vis. Pattern Recog.*, pages 19702–19712, 2023. 6
- [15] Qing Jiang, Yuqin Yang, Yuda Xiong, Yihao Chen, Zhaoyang Zeng, Tianhe Ren, Lei Zhang, et al. ChatRex: Taming multimodal LLM for joint perception and understanding. *arXiv preprint arXiv:2411.18363*, 2024. 3, 8
- [16] Feng Li, Hao Zhang, Shilong Liu, Jian Guo, Lionel M Ni, and Lei Zhang. DN-DETR: Accelerate detr training by introducing query denoising. In *IEEE Conf. Comput. Vis. Pattern Recog.*, pages 13619–13627, 2022. 3
- [17] Liunian Harold Li, Pengchuan Zhang, Haotian Zhang, Jianwei Yang, Chunyuan Li, Yiwu Zhong, Lijuan Wang, Lu Yuan, Lei Zhang, Jenq-Neng Hwang, et al. Grounded language-image pre-training. In *IEEE Conf. Comput. Vis. Pattern Recog.*, pages 10965–10975, 2022. 2, 3
- [18] Chuang Lin, Yi Jiang, Lizhen Qu, Zehuan Yuan, and Jianfei Cai. Generative region-language pretraining for open-ended object detection. In *IEEE Conf. Comput. Vis. Pattern Recog.*, pages 13958–13968, 2024. 2, 3, 8
- [19] Tsung-Yi Lin, Michael Maire, Serge Belongie, James Hays, Pietro Perona, Deva Ramanan, Piotr Dollár, and C Lawrence Zitnick. Microsoft coco: Common objects in context. In *Eur. Conf. Comput. Vis.*, pages 740–755, 2014. 2, 6
- [20] Shilong Liu, Feng Li, Hao Zhang, Xiao Yang, Xianbiao Qi, Hang Su, Jun Zhu, and Lei Zhang. DAB-DETR: Dynamic anchor boxes are better queries for detr. In *Int. Conf. Learn. Represent.* 3
- [21] Shilong Liu, Tianhe Ren, Jiayu Chen, Zhaoyang Zeng, Hao Zhang, Feng Li, Hongyang Li, Jun Huang, Hang Su, Jun Zhu, et al. Detection transformer with stable matching. In *Int. Conf. Comput. Vis.*, pages 6491–6500, 2023. 3
- [22] Shilong Liu, Zhaoyang Zeng, Tianhe Ren, Feng Li, Hao Zhang, Jie Yang, Chunyuan Li, Jianwei Yang, Hang Su, Jun Zhu, et al. Grounding DINO: Marrying DINO with grounded pre-training for open-set object detection. *Eur. Conf. Comput. Vis.*, 2024. 2, 3, 4, 5, 6
- [23] Ze Liu, Yutong Lin, Yue Cao, Han Hu, Yixuan Wei, Zheng Zhang, Stephen Lin, and Baining Guo. Swin Transformer: Hierarchical vision transformer using shifted windows. In *Int. Conf. Comput. Vis.*, pages 10012–10022, 2021. 6
- [24] Lingchen Meng, Xiyang Dai, Jianwei Yang, Dongdong Chen, Yinpeng Chen, Mengchen Liu, Yi-Ling Chen, Zuxuan Wu, Lu Yuan, and Yu-Gang Jiang. Learning from rich semantics and coarse locations for long-tailed object detection. *Adv. Neural Inform. Process. Syst.*, 36:78082–78094, 2023. 3
- [25] Yifan Pu, Weicong Liang, Yiduo Hao, Yuhui Yuan, Yukang Yang, Chao Zhang, Han Hu, and Gao Huang. Rank-DETR

- for high quality object detection. *Adv. Neural Inform. Process. Syst.*, 36:16100–16113, 2023. 3, 6
- [26] Alec Radford, Jong Wook Kim, Chris Hallacy, Aditya Ramesh, Gabriel Goh, Sandhini Agarwal, Girish Sastry, Amanda Askell, Pamela Mishkin, Jack Clark, et al. Learning transferable visual models from natural language supervision. In *Int. Conf. Mach. Learn.*, pages 8748–8763, 2021. 4, 6
- [27] Shaoqing Ren, Kaiming He, Ross Girshick, and Jian Sun. Faster R-CNN: Towards real-time object detection with region proposal networks. *IEEE Trans. Pattern Anal. Mach. Intell.*, 39(6):1137–1149, 2017. 2, 3, 6
- [28] Hamid Rezaatofghi, Nathan Tsoi, JunYoung Gwak, Amir Sadeghian, Ian Reid, and Silvio Savarese. Generalized intersection over union: A metric and a loss for bounding box regression. In *IEEE Conf. Comput. Vis. Pattern Recog.*, pages 658–666, 2019. 6
- [29] Tal Ridnik, Emanuel Ben-Baruch, Nadav Zamir, Asaf Noy, Itamar Friedman, Matan Protter, and Lihi Zelnik-Manor. Asymmetric loss for multi-label classification. In *Int. Conf. Comput. Vis.*, pages 82–91, 2021. 5, 6
- [30] T-YLPG Ross and GKHP Dollár. Focal loss for dense object detection. In *IEEE Conf. Comput. Vis. Pattern Recog.*, pages 2980–2988, 2017. 2, 3, 6, 8
- [31] Shuai Shao, Zeming Li, Tianyuan Zhang, Chao Peng, Gang Yu, Xiangyu Zhang, Jing Li, and Jian Sun. Objects365: A large-scale, high-quality dataset for object detection. In *Int. Conf. Comput. Vis.*, pages 8430–8439, 2019. 2, 3
- [32] Jingru Tan, Changbao Wang, Buyu Li, Quanquan Li, Wanli Ouyang, Changqing Yin, and Junjie Yan. Equalization loss for long-tailed object recognition. In *IEEE Conf. Comput. Vis. Pattern Recog.*, pages 11662–11671, 2020. 3
- [33] Jingru Tan, Xin Lu, Gang Zhang, Changqing Yin, and Quanquan Li. Equalization loss v2: A new gradient balance approach for long-tailed object detection. In *IEEE Conf. Comput. Vis. Pattern Recog.*, pages 1685–1694, 2021. 3
- [34] Gemini Team, Rohan Anil, Sebastian Borgeaud, Jean-Baptiste Alayrac, Jiahui Yu, Radu Soricut, Johan Schalkwyk, Andrew M Dai, Anja Hauth, Katie Millican, et al. Gemini: a family of highly capable multimodal models. *arXiv preprint arXiv:2312.11805*, 2023. 3
- [35] Zhi Tian, Chunhua Shen, Hao Chen, and Tong He. FCOS: A simple and strong anchor-free object detector. *IEEE Trans. Pattern Anal. Mach. Intell.*, 44(4):1922–1933, 2022. 3, 6
- [36] Jiaqi Wang, Wenwei Zhang, Yuhang Zang, Yuhang Cao, Jiangmiao Pang, Tao Gong, Kai Chen, Ziwei Liu, Chen Change Loy, and Dahua Lin. Seesaw loss for long-tailed instance segmentation. In *IEEE Conf. Comput. Vis. Pattern Recog.*, pages 9695–9704, 2021. 3
- [37] Jiaqi Wang, Pan Zhang, Tao Chu, Yuhang Cao, Yujie Zhou, Tong Wu, Bin Wang, Conghui He, and Dahua Lin. V3Det: Vast vocabulary visual detection dataset. In *Int. Conf. Comput. Vis.*, pages 19844–19854, 2023. 2, 3, 5, 6, 8
- [38] Jiaqi Wang, Yuhang Zang, Pan Zhang, Tao Chu, Yuhang Cao, Zeyi Sun, Ziyu Liu, Xiaoyi Dong, Tong Wu, Dahua Lin, et al. V3det challenge 2024 on vast vocabulary and open vocabulary object detection: Methods and results. *arXiv preprint arXiv:2406.11739*, 2024. 3
- [39] Yingming Wang, Xiangyu Zhang, Tong Yang, and Jian Sun. Anchor DETR: Query design for transformer-based detector. In *Proc. AAAI Conf. Artif. Intell.*, pages 2567–2575, 2022. 3
- [40] Junfeng Wu, Yi Jiang, Qihao Liu, Zehuan Yuan, Xiang Bai, and Song Bai. General object foundation model for images and videos at scale. In *IEEE Conf. Comput. Vis. Pattern Recog.*, pages 3783–3795, 2024. 3
- [41] Hao Yang, Hao Wu, and Hao Chen. Detecting 11k classes: Large scale object detection without fine-grained bounding boxes. In *Int. Conf. Comput. Vis.*, pages 9805–9813, 2019. 3
- [42] Jianwei Yang, Chunyuan Li, Xiyang Dai, and Jianfeng Gao. Focal modulation networks. *Adv. Neural Inform. Process. Syst.*, 35:4203–4217, 2022. 3
- [43] Lewei Yao, Jianhua Han, Youpeng Wen, Xiaodan Liang, Dan Xu, Wei Zhang, Zhenguo Li, Chunjing Xu, and Hang Xu. DetCLIP: Dictionary-enriched visual-concept paralleled pre-training for open-world detection. *Adv. Neural Inform. Process. Syst.*, 35:9125–9138, 2022. 3
- [44] Licheng Yu, Patrick Poirson, Shan Yang, Alexander C Berg, and Tamara L Berg. Modeling context in referring expressions. In *Eur. Conf. Comput. Vis.*, pages 69–85, 2016. 2
- [45] Alireza Zareian, Kevin Dela Rosa, Derek Hao Hu, and Shih-Fu Chang. Open-Vocabulary object detection using captions. In *IEEE Conf. Comput. Vis. Pattern Recog.*, pages 14393–14402, 2021. 2
- [46] Hao Zhang, Feng Li, Shilong Liu, Lei Zhang, Hang Su, Jun Zhu, Lionel Ni, and Heung-Yeung Shum. DINO: DETR with improved denoising anchor boxes for end-to-end object detection. In *Int. Conf. Learn. Represent.*, 2023. 3, 6, 7, 8
- [47] Shifeng Zhang, Cheng Chi, Yongqiang Yao, Zhen Lei, and Stan Z Li. Bridging the gap between anchor-based and anchor-free detection via adaptive training sample selection. In *IEEE Conf. Comput. Vis. Pattern Recog.*, pages 9759–9768, 2020. 6
- [48] Yuanhan Zhang, Qinghong Sun, Yichun Zhou, Zexin He, Zhenfei Yin, Kun Wang, Lu Sheng, Yu Qiao, Jing Shao, and Ziwei Liu. Bamboo: Building mega-scale vision dataset continually with human-machine synergy. *arXiv preprint arXiv:2203.07845*, 2022. 2
- [49] Zhilu Zhang and Mert Sabuncu. Generalized cross entropy loss for training deep neural networks with noisy labels. *Adv. Neural Inform. Process. Syst.*, 31, 2018. 3
- [50] Yaochi Zhao, Sen Chen, Shiguang Liu, Zhuhua Hu, and Jingwen Xia. Hierarchical equalization loss for long-tailed instance segmentation. *IEEE Trans. Multimedia*, 26:6943–6955, 2024. 3
- [51] Yiwu Zhong, Jianwei Yang, Pengchuan Zhang, Chunyuan Li, Noel Codella, Liunian Harold Li, Luowei Zhou, Xiyang Dai, Lu Yuan, Yin Li, et al. RegionCLIP: Region-based language-image pretraining. In *IEEE Conf. Comput. Vis. Pattern Recog.*, pages 16793–16803, 2022. 3
- [52] Xingyi Zhou, Vladlen Koltun, and Philipp Krähenbühl. Probabilistic two-stage detection. *arXiv preprint arXiv:2103.07461*, 2021. 6
- [53] Xingyi Zhou, Rohit Girdhar, Armand Joulin, Philipp Krähenbühl, and Ishan Misra. Detecting twenty-thousand classes using image-level supervision. In *Eur. Conf. Comput. Vis.*, pages 350–368. Springer, 2022. 3

- [54] Xizhou Zhu, Weijie Su, Lewei Lu, Bin Li, Xiaogang Wang, and Jifeng Dai. Deformable DETR: Deformable transformers for end-to-end object detection. In *Int. Conf. Learn. Represent.*, 2021. [3](#), [6](#)